The American Journal of Pathology, Vol. 175, No. 1, July 2009

DOI: 10.2353/ajpath.2009.080908

Short Communication

Involvement of WAVE Accumulation in Aβ/APP Pathology-Dependent Tangle Modification in Alzheimer's Disease

Kazuyuki Takata,* Yoshihisa Kitamura,* Yukinori Nakata,* Yasuji Matsuoka,† Hidekazu Tomimoto,‡ Takashi Taniguchi,* and Shun Shimohama§

From the Department of Neurobiology and 21st Century COE Program, Kyoto Pharmaceutical University, Misasagi, Yamashina-ku, Kyoto, Japan; the Department of Neurology,† Georgetown University Medical Center, Washington, DC; the Department of Neurology,‡ Mie University, Graduate School of Medicine, Tsu, Japan; and the Department of Neurology,§ Sapporo Medical University, School of Medicine, Sapporo, Japan*

Synaptic deficits are closely correlated with cognitive dysfunction in Alzheimer's disease (AD), and synaptic integrity is regulated by the actin cytoskeleton. We demonstrated here that the Wiskott-Aldrich syndrome protein family verprolin-homologous protein (WAVE), a key molecule for actin assembly, co-aggregated with both hyperphosphorylated tau and phosphorylated collapsin response mediator protein 2 (CRMP2) in neurofibrillary tangles and abnormal neurites of the AD brain. Although phosphorylated CRMP2 accumulation was induced in the brains of JNPL3 mice, WAVE accumulation was not detected in the brains of either JNPL3 or Tg2576 mice that developed neurofibrillary tangles and amyloid-β (Aβ) plaques, respectively. Interestingly, both phosphorylated CRMP2 accumulation and WAVE accumulation were recapitulated in the brains of 3xTg-AD mice that developed neurofibrillary tangles and Aβ plaques. In addition, we found an interaction between WAVE, CRMP2, and hyperphosphorylated tau in the cytosolic fraction of the AD brain. Taken together, WAVE accumulation may require both Aβ/amyloid precursor protein and tau pathologies, and an interaction between WAVE, CRMP2, and hyperphosphorylated tau may be involved in this process. Thus, WAVE accumulation may be involved in Aβ/amyloid precursor protein mediated-tangle modification, suggesting a possible correlation between WAVE accumulation and synaptic deficits induced by disturbances in actin assembly in AD brains. ***(Am J Pathol 2009, 175:17–24; DOI: 10.2353/ajpath.2009.080908)***

The pathological hallmarks of Alzheimer's disease (AD) include senile plaques, neurofibrillary tangles (NFTs), synaptic loss, and neurodegeneration.[1] Senile plaques are formed by the accumulation of extracellular amyloid-β (Aβ), which is generated from the amyloid precursor protein (APP), and NFTs are composed of paired helical filaments (PHFs) in neuronal perikarya. Minute bundles of PHFs are found in dendrites as neuropil threads (curly fibers) and in axonal terminals as dystrophic neurites surrounding senile plaques. The main component of PHFs has been identified as abnormally hyperphosphorylated tau protein.[2] Tau is a microtubule-associated protein; therefore, one component in the developmental cascade of AD may include a disturbance of microtubule cytoskeleton.[3]

The formation of abnormal neurites such as neuropil threads and dystrophic neurites in AD brains is associated with aberrant neuritic sprouting.[4] Neuritic sprouting is critically dependent on the interplay between microtu-

Supported by grants of the 21st Century Center of Excellence and Frontier Research Programs from the Ministry of Education, Culture, Sports, Science and Technology of Japan; a grant from Japan Society for the Promotion of Science; and grants from National Institute of Health (AG026478 and AG022455) (to Y.M.).

Accepted for publication March 19, 2009.

Y.K. and S.S. both served as senior authors.

Supplemental material for this article can be found on *http://ajp.amjpathol.org.*

Current address of Y.M.: Neurodegeneration Research, GlaxoSmithKline, Shanghai 201203, China.

Address reprint requests to Yoshihisa Kitamura, Ph.D., Department of Neurobiology and 21st Century COE Program, Kyoto Pharmaceutical University, Misasagi, Yamashina-ku, Kyoto 607-8414, Japan. E-mail: yokita@mb.kyoto-phu.ac.jp, or Shun Shimohama, M.D., Ph.D., Department of Neurology, Sapporo Medical University, School of Medicine, S1W16, Chuo-ku, Sapporo 060-8543, Japan. E-mail: shimoha@sapmed.ac.jp.

bule and actin cytoskeletons.[5] Furthermore, synaptic integrity is maintained by the precise formation of dendritic spines that are major sites of synaptic contacts, and the formation is structurally regulated by the actin cytoskeleton.[6] On the other hand, progressive synaptic dysfunction is found in AD brains and closely correlates with cognitive deficits.[7] Thus, the disruption of the actin cytoskeleton, as well as the disturbance of microtubule assembly are suggested to be involved in the developmental cascade in AD. However, the relationship between disruptions of microtubule and actin cytoskeletons and the involvement of Aβ/APP and tau pathologies in actin cytoskeletal disturbance in AD remain poorly understood.

Recently, Wiskott-Aldrich syndrome protein family verprolin-homologous protein (WAVE) has been identified as a key molecule for actin assembly,[8] and WAVE knockout mice demonstrated the association between WAVE dysfunction and impaired learning and memory.[9,10] In addition, collapsin response mediator protein 2 (CRMP2) regulates microtubule assembly in neurons.[11] A recent study has reported that CRMP2 interacts with the specifically Rac1-associated protein 1/WAVE complex, and transports WAVE into the axonal growth cones.[12] Thus, CRMP2 and WAVE seem to be mediators required in the cross talk between microtubule and actin cytoskeletons. Previous studies have demonstrated that CRMP2 is highly phosphorylated and is associated with NFTs and abnormal neurites in AD brains.[13,14] In this context, the abnormality of CRMP2 possibly influences the property of WAVE and furthermore actin assembly.

Materials and Methods

Human Materials and Preparation of Brain Section

All experiments using human materials were performed in accordance with the guidelines of ethical committees of Kyoto Pharmaceutical University. Informed consent was obtained from all subjects. The tissue of frontal cortices from a patient who was clinically and histopathologically diagnosed as AD (age; 67-year-old, CERAD criteria; C, Braak stage; IV), and a control (age; 77-year-old, CERAD criteria; A, Braak stage; I) with no clinical or morphological evidence of brain pathology were used. The dissected tissue blocks were fixed in 10% formalin and were cut into 20-μm sections on a cryostat.

Preparation of Sarkosyl-Insoluble Fraction

Temporal cortices from four AD patients and four controls were homogenized in 10 mmol/L HEPES buffer (pH 7.0) containing 0.32 M/L sucrose, 0.05% NaN_3, and cocktails of protease inhibitors and phosphatase inhibitors as described previously.[15] After centrifugation at 12,000 $\times$ *g* for 30 minutes, the supernatants were collected as the cytosol fraction and the resulting precipitates were used for the preparation of the sarkosyl-insoluble fraction, which is enriched in PHFs, as described previously.[16] Briefly, the precipitates were washed three times with the same homogenization buffer, and then protein concentrations were measured. Three milligrams of proteins were re-homogenized in 500 μl of the homogenization buffer and one-tenth volume of 10% sarkosyl solution was added. The homogenates were mixed by vortex, and then incubated for 1 hour at 37°C. After centrifugation at 100,000 $\times$ *g* for 1 hour, the pellets were dissolved in 50 μl of Laemmli's sample buffer and analyzed as the sarkosyl-insoluble fractions.

Animals

Triple transgenic mice (3xTg-AD) expressing human Swedish double-mutated APP $(APP)_{swe}$, human mutated four-repeat tau (tau_{P301L}), and human mutated presenilin 1 ($PS1_{M146V}$) were originally generated by Oddo and colleagues.[17] Hemizygous Tg2576 mice expressing APP_{swe}[18] and hemizygous JNPL3 mice expressing tau_{P301L}[19] were purchased from Taconic (Germantown, NY). Only female mice were used in this study. All animal experiments were approved by the Committee for Animal Research at Kyoto Pharmaceutical University and the Animal Care and Use Committee of Georgetown University Medical Center. Mice were sacrificed by cervical dislocation and brains were immersion fixed in 4% paraformaldehyde. The cryoprotected brain blocks were cut into 20-μm sections on a cryostat.

Immunohistochemistry

The free-floating human brain sections and mouse brain sections were incubated with an antibody against Aβ (clone 6E10, epitope; aa. 3 to 8 of Aβ, 1:1000, Chemicon, Temecula, CA), phosphorylated tau (clone AT8, epitope; phosphorylated Ser202 and phosphorylated Thr205 of tau, 1:3000, Innogenetics, Gent, Belgium), phosphorylated CRMP2 (clone 3F4, epitope; phosphorylated Thr509 and phosphorylated Ser522 of CRMP2, 1:100, IBL, Gunma, Japan), or WAVE (H-180, immunogen; aa. 1-180 of human WAVE1, 1:100, Santa Cruz, Santa Cruz, CA). The clone 6E10 antibody reacts with APP, secreted APP, C-terminal fragments of APP and Aβ (Aβ/APP). Sections were then incubated with a biotinylated anti-mouse or anti-rabbit IgG antibody (1:2000, Vector Laboratories, Burlingame, CA), and followed by the incubation with avidin peroxidase (ABC Elite Kit, 1:4000, Vector Laboratories). Subsequently, the labeling was visualized by incubation with 50 mmol/L Tris-HCl buffer (pH 7.6) containing 0.02% 3,3′-diaminobenzidine and 0.0045% hydrogen peroxide with nickel enhancement.

Laser Confocal Microscopy

Sections were co-incubated with rabbit polyclonal anti-WAVE antibody (H-180, 1:100) and mouse monoclonal anti-phosphorylated tau antibody (clone AT8, 1:3000) or mouse monoclonal anti-phosphorylated CRMP2 antibody (clone 3F4, 1:100); or rabbit polyclonal anti-phosphorylated tau antibody (pThr205, epitope: phosphorylated

Thr205 of tau, 1:1000, Sigma, Saint Louis, MO) and mouse monoclonal phosphorylated CRMP2 antibody (clone 3F4, 1:100). In the semiquantitative analysis described below, the immunoreactive area of clone AT8 antibody was corresponded to that of pThr205 (99.5 ± 6.9%) in the AD brain. The primary antibodies were then probed with Alexa Fluor 546-labeled anti-mouse IgG antibody and Alexia Fluor 488-labeled anti-rabbit IgG antibody (each diluted 1:500, Invitrogen, Carlsbad, CA). For the thioflavin S staining, brain sections mounted on glass slides were incubated with 1% thioflavin S solution in 70% ethanol, and then rinsed with 70%, 95%, and 100% ethanol. Subsequently, fluorescence was detected using a laser scanning confocal microscope (LSM510META, Carl Zeiss, Jena, Germany). Semiquantitative image analysis of immunoreactive area was performed as described previously[20] using the software WinRoof (Mitani, Fukui, Japan). For z-axis scanning, images of 1-μm confocal z-series were acquired, and the images obtained were reconstructed with the software ImageBrowser (Carl Zeiss).

Western Blotting

Western blotting was performed as described previously.[15] The cytosol fraction and sarkosyl-insoluble fractions were subjected to sodium dodecyl sulfate polyacrylamide gel electrophoresis. Immunoblotting was performed by transferring proteins from the slab gel to a sheet of polyvinylidene difluoride membrane by electroelution. The membrane was incubated with antibody against phosphorylated tau (clone AT8; 1:200), caspase-3 (clone 19/Caspase-3/CPP32, immunogen; aa. 1-219 of human CPP32, 1:1000, BD Bioscience, San Jose, CA), CRMP2 (clone C4G, immunogen; aa. 486-528 of CRMP2, 1:100, IBL), or WAVE (H-180, 1:1000), followed by the horseradish peroxidase-conjugated secondary antibody (each diluted 1:1000, GE Health care, Buckinghamshire, UK). The bound horseradish peroxidase-labeled antibodies were detected by chemiluminescence (ECL kit, GE Health care).

Immunoprecipitation

Cytosol fraction from the AD brain was mixed with 10 μl of protein G-Sepharose (GE Health care) and 5 μg of IgG of an antibody against Aβ/APP (clone 6E10), phosphorylated tau (clone AT8), non-phosphorylated tau (clone Tau1, epitope; non-phosphorylated Ser199 and non-phosphorylated Ser202, Chemicon), total tau (clone Tau5, immunogen; middle aa. sequence of bovine tau, Chemicon), WAVE (H-180), or α-synuclein (clone 42, immunogen: aa. 15-123 of rat synuclein-1, BD Biosciences). After the incubation for 3 hours at 4°C, mixture was centrifuged at 10,000 × *g* for 10 minutes. The precipitates washed were boiled for 5 minutes in Laemmli's sample buffer. Aliquots were run on polyacrylamide gels and subjected to Western blotting with antibody against CRMP2 (clone C4G, 1:100), non-phosphorylated tau (clone Tau1, 1:500), or phosphorylated tau (clone AT8, 1:200).

Results

Accumulation of WAVE in AD Brain

Localization of WAVE in non-dementia and AD brains was compared with that of hyperphosphorylated tau and phosphorylated CRMP2. Accumulation of hyperphosphorylated tau (Figure 1A) was detected in NFTs (black arrow), neuropil threads (black arrowheads), and dystrophic neurites (white arrowheads) in the frontal cortex of the AD brain, but not in the non-dementia brain. Consistent with a previous study,[13] phosphorylated CRMP2 (Figure 1B) was accumulated in NFTs (black arrows), neuropil threads (black arrowheads), and dystrophic neurites (white arrowheads) of the AD brain. However, no significant staining was observed in the non-dementia brain. WAVE immunoreactivity (Figure 1C) was faintly and diffusely observed in the non-dementia brain parenchyma. In the AD brain, distinct intraneuronal accumulation of WAVE was detected in structures resembling NFTs (black arrows), neuropil threads (black arrowheads), and dystrophic neurites (white arrowheads).

In the laser confocal microscopic analysis, we found that WAVE co-localized with hyperphosphorylated tau (Figure 1D) and phosphorylated CRMP2 (Figure 1E) in NFTs, neuropil threads, and dystrophic neurites in the AD brain. Hyperphosphorylated tau and phosphorylated CRMP2 were also co-localized in the AD brain (Figure 1F). Semiquantitative image analysis revealed that 70.0 ± 7.7% of hyperphosphorylated τ- or 75.9 ± 4.4% of phosphorylated CRMP2-immunoreactive structures contained WAVE immunoreactivity (Figure 1, G and H, respectively), and 89.2 ± 4.7% of hyperphosphorylated τ-immunoreactive structures contained phosphorylated CRMP2 (Figure 1I). Thus, immunoreactive area was larger in the order of hyperphosphorylated tau, phosphorylated CRMP2, and WAVE in the AD brain.

WAVE Accumulation in the Sarkosyl-Insoluble Fraction and Interaction of CRMP2, Tau, and WAVE in the Cytosol Fraction of the AD Brain

We prepared sarkosyl-insoluble fractions from non-dementia and AD brains. To confirm the fractionation, we first examined the detection of hyperphosphorylated tau as a positive control and caspase-3, a soluble cytosol protein, as a negative control for the sarkosyl-insoluble fraction from the AD brain (Figure 2A). Although the amount of hyperphosphorylated tau in the sarkosyl-insoluble fraction was greater than that in the cytosol fraction, caspase-3 was only detected in the cytosol fraction of the AD brain. Thus, PHFs-associated proteins were enriched in the sarkosyl-insoluble fraction. In these sarkosyl-insoluble fractions, we detected hyperphosphorylated tau, CRMP2, and WAVE in AD brains, but not in non-dementia brains (Figure 2B). Taken together, the above studies

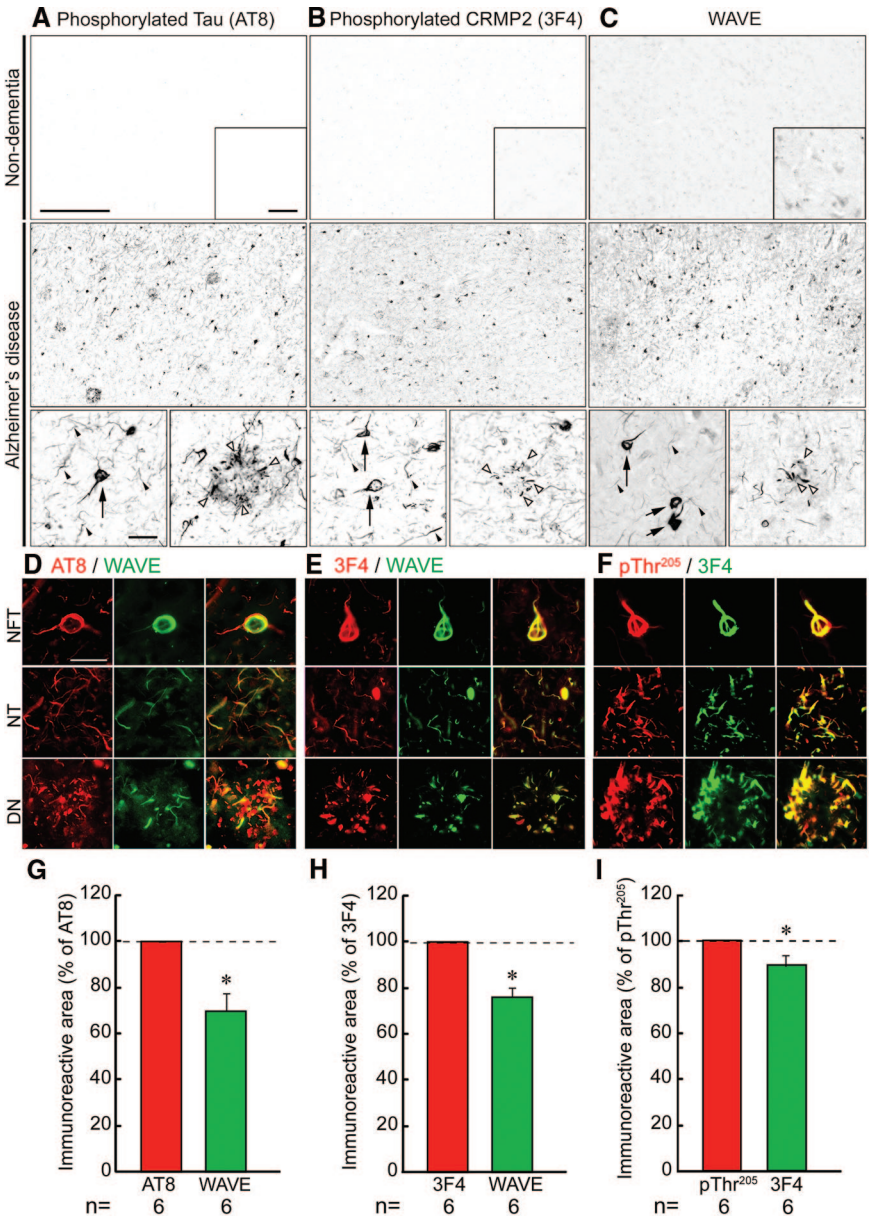

Figure 1. Localization of WAVE in the frontal cortex of non-dementia and AD. **A:** Although no hyperphosphorylated tau was detected in the non-dementia brain, marked accumulation of hyperphosphorylated tau was detected in NFTs and abnormal neurites in the AD brain. **B:** No immunoreactivity of phosphorylated CRMP2 was detected in the non-dementia brain, whereas marked accumulation of phosphorylated CRMP2 was found in NFTs and abnormal neurites in the AD brain. **C:** Faint WAVE immunoreactivity was observed throughout the brain parenchyma and moderate immunoreactivity was detected in neuronal perikarya of the non-dementia brain. On the other hand, intraneuronal accumulation of WAVE was detected in NFTs- and abnormal neurites-like structures of the AD brain. **Inset** shows high magnification of each panel. Scale bars in **A–C** = 500 μm (**upper** and **middle panels**), 50 μm (**inset**), and 50 μm (**lower panel**). **Arrows**, **black arrowheads**, and **white arrowheads** indicate NFTs, neuropil threads, and dystrophic neurites, respectively. **D–F:** In the confocal microscopic analysis, WAVE (**D** and **E**; green) was co-localized with hyperphosphorylated tau (clone AT8; **D**; red) or phosphorylated CRMP2 (clone 3F4; **E**; red) in neurons of the AD brain. In addition, hyperphosphorylated tau (pThr205; **F**; red) was also co-localized with phosphorylated CRMP2 (clone 3F4; **F**; green). NFT: neurofibrillary tangle, NT: neuropil threads, DN: dystrophic neurites. Scale bars in **D** = 20 μm for all panels in **D–F**. **G–I:** In the semiquantitative image analysis, the immunoreactive areas of hyperphosphorylated tau (clone AT8) and WAVE; phosphorylated CRPM2 (clone 3F4) and WAVE; or hyperphosphorylated tau (pThr205) and phosphorylated CRMP2 (clone 3F4) were measured using the images taken by the confocal microscopic analysis, and then standardized with the areas of AT8, 3F4, and pThr205 respectively. Results were given as mean ± SEM. The statistical significance of differences was determined by student's *t*-test. $^*P < 0.05$ in **G**, **H**, and **I** vs. the value in AT8, 3F4, and pThr205 respectively.

suggest that hyperphosphorylated tau, CRMP2, and WAVE are co-aggregated in NFTs and abnormal neurites in AD brains.

We next examined the interaction of CRMP2 with Aβ/APP, tau, or WAVE in the AD brain by immunoprecipitation (Figure 2C). An approximately 62-kDa band of CRMP2 was detected in the AD cytosol fraction. This band was also detected in the AD cytosol fraction immunoprecipitated by the antibody against hyperphosphorylated tau (clone AT8), non-phosphorylated tau (clone Tau1), total tau (clone Tau5) or WAVE, but not by the antibody against Aβ/APP (clone 6E10) or α-synuclein. Thus, CRMP2 appears to interact with tau and WAVE, and its affinity for hyperphosphorylated tau seems to be stronger than non-phosphorylated tau. We further examined the interaction of WAVE with non-phosphorylated tau or hyperphosphorylated tau. In the AD cytosol fraction immunoprecipitated with anti-WAVE antibody, whose volume is three times as much as that used for the CRMP2 detection (Figure 2C), hyperphosphorylated tau (Figure 2E), but not non-phosphorylated tau (Figure 2D), was slightly detected. Thus, WAVE faintly associated with hyperphosphorylated tau in the cytosol fraction of the AD brain. This result suggests that WAVE and tau may interact with each other through CRMP2, and stronger affinity of CRMP2 for hyperphosphorylated tau than non-phosphorylated tau may allow us to detect the slight interaction of hyperphosphorylated tau to WAVE.

CRMP2 and WAVE Pathologies in JNPL3 Mice, Tg2576 Mice, and 3xTg-AD Mice

To examine the effects of hyperphosphorylated tau and Aβ/APP on the CRMP2 and WAVE pathologies, we first

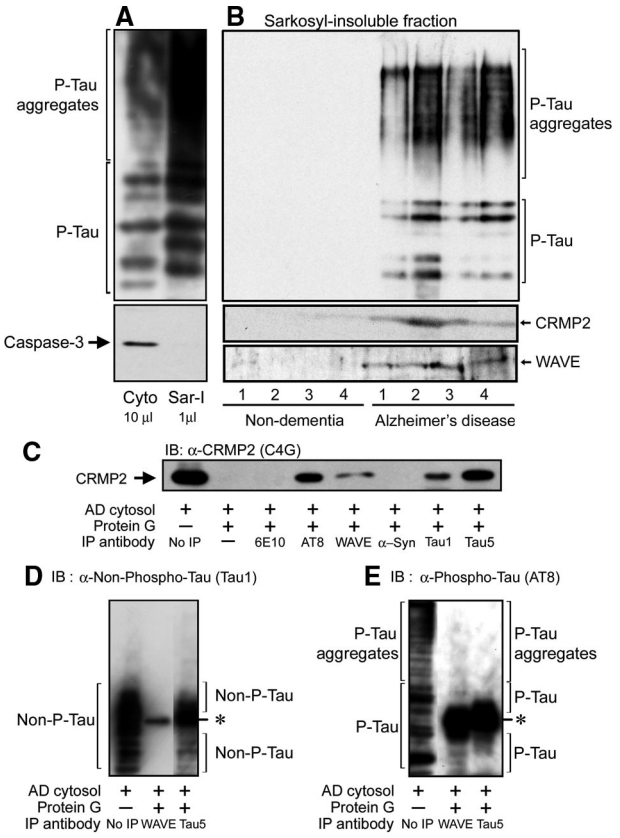

Figure 2. WAVE accumulation in the sarkosyl-insoluble fraction and interaction of CRMP2, tau, and WAVE in the cytosol fraction of the AD brain. **A:** Although the amount of hyperphosphorylated tau in the sarkosyl-insoluble fraction was greater than that in the cytosol fraction, caspase-3 was only detected in the cytosol fraction of the AD brain. Thus, PHFs-associated proteins were enriched in the sarkosyl-insoluble fraction. **B:** In the sarkosyl-insoluble fractions, hyperphosphorylated tau, CRMP2, and WAVE were detected in AD brains, but not in non-dementia brains. **C:** Ten microliters of immunoprecipitated samples of the AD cytosol fraction were run on the gel, and blotted with anti-CRMP2 antibody (clone C4G). CRMP2 immunoreactivity was detected in the AD cytosol fraction immunoprecipitated by the antibody against hyperphosphorylated tau (clone AT8), non-phosphorylated tau (clone Tau1), total tau (clone Tau5) or WAVE, but not in that immunoprecipitated by the antibody against Aβ/APP (clone 6E10) or α-synuclein. **D** and **E:** Thirty microliters or 2 μl of the AD cytosol fraction immunoprecipitated with antibody against WAVE or total tau (clone Tau5), respectively, were run on the gel, and blotted with antibody against non-phosphorylated tau (clone Tau1; **D**) or phosphorylated tau (clone AT8; **E**). **D:** No immunoreactivity of non-phosphorylated tau was detected in the AD cytosol fraction immunoprecipitated with anti-WAVE antibody. In the AD cytosol fraction immunoprecipitated with Tau5 antibody, a smear band of non-phosphorylated tau was detected. **E:** In the AD cytosol fraction immunoprecipitated with anti-WAVE antibody or Tau5 antibody, a smear band of phosphorylated tau was slightly detected. P-Tau and Phospho-Tau: phosphorylated tau, Non-phospho-Tau and Non-P-Tau: non-phosphorylated tau, α-Syn: α-synuclein, IP: immunoprecipitation, IB: immunoblotting. *nonspecific bands of IgGs used for the immunoprecipitation.

analyzed brains of aged JNPL3 mice and Tg2576 mice. In 16-month-old JNPL3 mice, although no Aβ/APP accumulation was observed (Figure 3A), marked accumulation of hyperphosphorylated tau (Figure 3B) and phosphorylated CRMP2 (Figure 3C) was detected in neurons of the hippocampus. While diffuse WAVE immunoreactivity was observed throughout the hippocampal parenchyma, no intraneuronal accumulation of WAVE was detected in JNPL3 mice (Figure 3D). In 20-month-old Tg2576 mice, marked extracellular deposits of Aβ/APP were formed in the hippocampus (Figure 3E). However, no intraneuronal accumulations of hyperphosphorylated tau (Figure 3F), phosphorylated CRMP2 (Figure 3G), and WAVE (Figure 3H) were detected. Similar results above were also detected in the amygdala and cortex (see supplemental Figure S1 at *http://ajp.amjpathol.org*).

We further analyzed brains of 3xTg-AD mice. In the hippocampus (Figure 3I) and amygdala (see supplemental Figure S2A at *http://ajp.amjpathol.org*), accumulation of intraneuronal Aβ/APP was detected at 10 months of age, and extracellular deposits of Aβ/APP were formed at 16 months and 21 months of age. Hyperphosphorylated tau and phosphorylated CRMP2 were detected in the neurons of the hippocampus (Figure 3, J and K) and amygdala (see supplemental Figure S2, B and C at *http://ajp.amjpathol.org*) at 16 months and 21 months, but not at 10 months of age. Furthermore, intraneuronal accumulation of WAVE was found weakly at 16 months and distinctly at 21 months of age in the hippocampus (Figure 3L) and amygdala (see supplemental Figure S2D at *http://ajp.amjpathol.org*). In the cerebral cortex of 3xTg-AD mice (see supplemental Figure S2E-H at *http://ajp.amjpathol.org*), intraneuronal accumulation of Aβ/APP was already present at 10 months of age, and diffuse extracellular deposition of Aβ/APP was detected at 16 and 21 months of age. However, no intraneuronal accumulations of hyperphosphorylated tau, phosphorylated CRMP2, and WAVE were detected. Thus, intraneuronal accumulations of phosphorylated CRMP2 and WAVE were induced in the brain regions where pathologies of Aβ/APP and tau occurred concurrently in aged 3xTg-AD mice.

We next performed three-dimensional image analysis in the hippocampus of 21-month-old 3xTg-AD mice. All intraneuronal accumulations of WAVE were found inside the hyperphosphorylated tau (Figure 3M)- or phosphorylated CRMP2 (Figure 3N)-immunoreactive neurons. These results further support the interaction of WAVE with hyperphosphorylated tau and CRMP2. We also found that all thioflavin S-positive NFTs contained WAVE immunoreactivity (Figure 3O). The number of WAVE-immunoreactive neurons was less than that of hyperphosphorylated τ- or phosphorylated CRMP2-immunoreactive neurons, while it was more than the number of neurons stained by thioflavin S (see supplemental Figure S2I at *http://ajp.amjpathol.org*).

In the JNPL3 mice, any WAVE accumulations were not detected. However, there is a possibility that the absence of WAVE accumulation is simply due to the lack of thioflavin S-positive NFTs in the hippocampus, amygdala, and cortex of JNPL3 mice. Therefore, we further analyzed the brain region where NFTs are abundant in JNPL3 mice.[19] In the brainstem of 16-month-old JNPL3 mice, although we found a lot of thioflavin S-positive NFTs and the co-localization of phosphorylated CRMP2 (see supplemental Figure S3D at *http://ajp.amjpathol.org*), no WAVE accumulation was detected (Figure 3P). In addition, we found a few thioflavin S-positive NFTs in the hippocampus, amygdala, and cortex of JNPL3 mice.

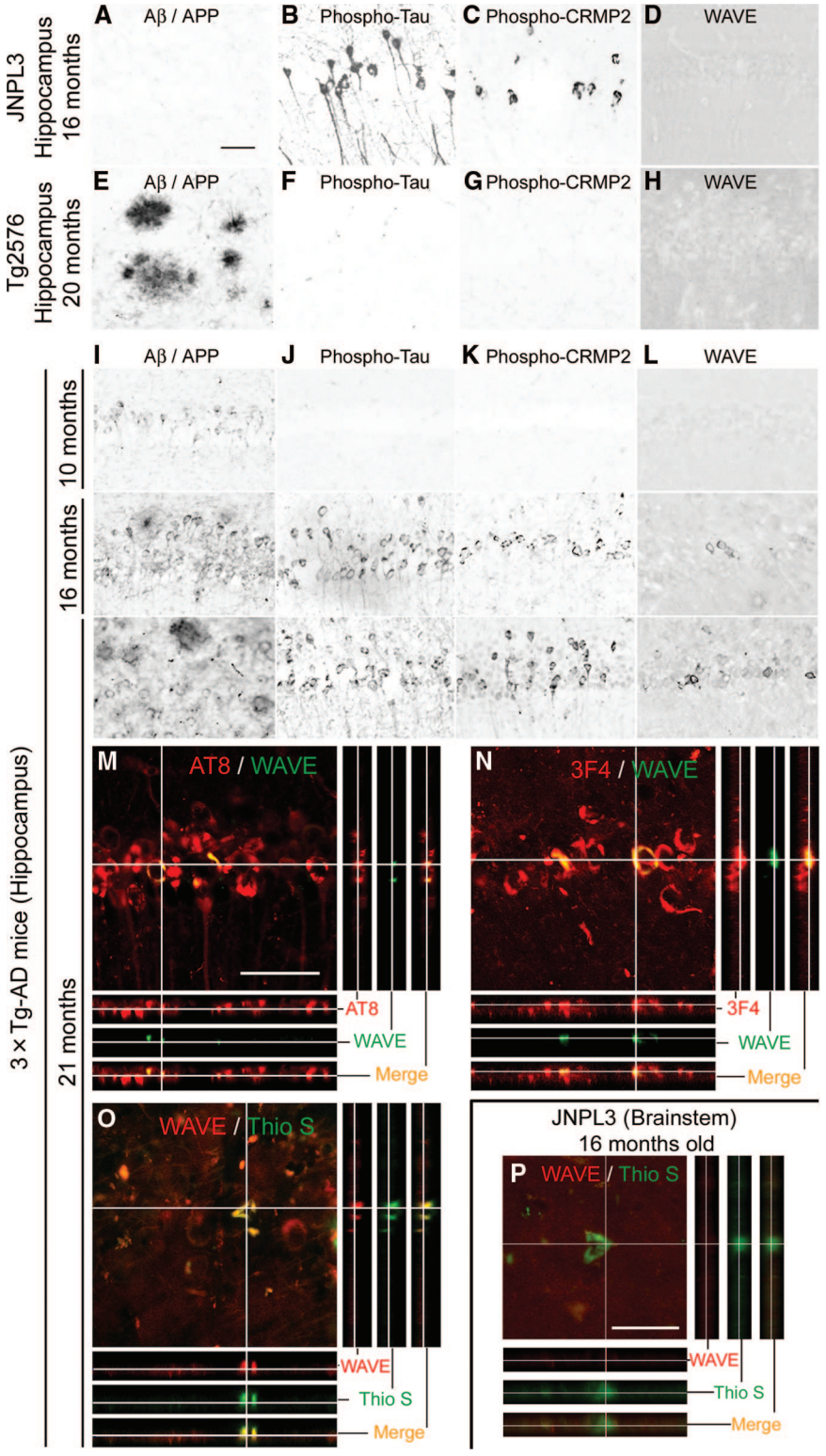

Figure 3. WAVE accumulation was induced in the brain regions where pathologies of Aβ/APP and tau occurred concurrently. In the hippocampus of JNPL3 mice (**A–D**), although no accumulation of Aβ/APP (clone 6E10) was detected (**A**), marked hyperphosphorylated tau accumulation (clone AT8) was observed in neurons (**B**). Intraneuronal accumulation of phosphorylated CRMP2 (clone 3F4) was also detected (**C**). Diffuse immunoreactivity of WAVE (H-180) but no intraneuronal accumulation was observed in the parenchyma (**D**). In the hippocampus of Tg2576 mice (**E–H**), marked extracellular deposition of Aβ/APP was observed (**E**). No intraneuronal accumulations of hyperphosphorylated tau (**F**) and phosphorylated CRMP2 (**G**) were detected. Diffuse immunoreactivity of WAVE but no intraneuronal accumulation was observed in the parenchyma (**H**). In the hippocampus of 3xTg-AD mice (**I–L**), intraneuronal accumulation of Aβ/APP was already observed at 10 months of age, and extracellular deposits of Aβ/APP were detected at 16 and 21 months of age (**I**). Hyperphosphorylated tau was accumulated in neurons at 16 and 21 months of age (**J**). Similarly, phosphorylated CRMP2 was accumulated at 16 and 21 months of age (**K**). In addition to the diffuse immunoreactivity of WAVE, intraneuronal accumulation of WAVE was found in neurons at 16 months and 21 months of age (**L**). **M–O:** Abnormal neurons in the hippocampus of 21-month-old 3xTg-AD mice were double-immunolabeled with antibodies against WAVE (green in **M** and **N**) and hyperphosphorylated tau (clone AT8; red in **M**) or phosphorylated CRMP2 (clone 3F4; red in **N**). Alternatively, abnormal neurons were immunolabeled with anti-WAVE antibody (red in **O**) and NFTs were counterstained with thioflavin S (Thio S; green in **O**). The different panels of views show the z-axis images re-constructed with the 1-μm confocal z-series. **P:** In the brainstem of 16-month-old JNPL3 mice, thioflavin S-positive NFTs (Thio S; green) were observed, WAVE immunoreactivity (red) was not detected. Scale bars shown in **A** = 50 μm for **A–L.** Scale bars shown in **M** and **P** = 50 μm for **M–P**.

However, we detected the intraneuronal accumulation of phosphorylated CRMP2 but not WAVE accumulation (see supplemental Figure S3 at *http://ajp.amjpathol.org*). Thus, WAVE accumulation was not detected in the thioflavin S-positive NFTs of the JNPL3 mice.

Discussion

In this study, we demonstrated intraneuronal accumulation of WAVE in the AD brain. In 16- and 21-month-old 3xTg-AD mice, intraneuronal WAVE accumulation was

recapitulated in the hippocampus and amygdala. The 3xTg-AD mice develop intraneuronal accumulations of Aβ/APP around 3 to 6 months of age[17] and the extracellular Aβ/APP plaques around 14 months of age in the hippocampus.[21] In contrast, pathology of hyperphosphorylated tau is apparent between 12 to 15 months of age.[17] We also detected the pathologies of Aβ/APP and hyperphosphorylated tau in the hippocampus and amygdala of 3xTg-AD mice at 16 and 21 months of age. Furthermore, in these regions, we found intraneuronal accumulation of WAVE. However, no WAVE accumulation was detected at the time when the pathology of Aβ/APP was only manifest (10 months of age) in 3xTg-AD mice. In addition, in the cerebral cortex of these mice, we could not detect any hyperphosphorylated tau or WAVE accumulations at all ages investigated in this study. Thus, single pathology of Aβ/APP is unlikely to induce WAVE accumulation, and the results of Tg2576 mice strongly support this notion. Although the oldest JNPL3 mouse examined in this study was 16 months of age due to its relatively short life span,[19] marked intraneuronal accumulation of hyperphosphorylated tau was detected in the hippocampus, amygdala, and cortex, and thioflavin S-positive NFTs were observed in the brainstem. However, a single transgene of human mutant tau did not induce the WAVE accumulation in JNPL3 mice. Thus, a combination of the pathologies of Aβ/APP and tau may be required for the intraneuronal accumulation of WAVE.

On the other hand, intraneuronal accumulation of phosphorylated CRMP2 was found in brain regions manifesting the pathology of hyperphosphorylated tau in JNPL3 mice and 3xTg-AD mice. However, no accumulation of phosphorylated CRMP2 was found in brain regions where only Aβ/APP pathology was detected in Tg2576 mice and 3xTg-AD mice. Thus, our results suggest that phosphorylated CRMP2 accumulation is initiated by the hyperphosphorylated tau. Likewise tau,[22] CRMP2 is sequentially phosphorylated by cyclin-dependent kinase 5 and glycogen synthase kinase 3β and then acquires the immunoreactivity for the clone 3F4 antibody.[23] Furthermore, the release of APP intracellular domain by γ-secretase seems to increase glycogen synthase kinase 3β activity and subsequently enhances the phosphorylation of CRMP2.[24] Cole and colleagues also reported that hyperphosphorylation of CRMP2 occurs in AD brains, which may be induced by processes leading to excessive Aβ generation, as an early event in the development of AD.[25] They further used 3xTg-AD mice and JNPL3 mice to examine the effect of the Aβ and tau pathologies on the CRMP2 phosphorylation by Western blot analysis and detected hyperphosphorylation of CRMP2 in 3xTg-AD mice but not in JNPL3 mice. Together with results in our immunohistochemistry, CRMP2 accumulated in neurons of 3xTg-AD mice may be hyperphosphorylated, whereas that in JNPL3 mice may be physiologically phosphorylated. Thus, the hyperphosphorylation and accumulation of CRMP2 may be initiated independently by processes in Aβ generation and hyperphosphorylated tau, respectively. In fact, the co-localization of Aβ/APP and tau pathologies was reported in NFTs[26] or synaptosomes of AD brain,[27] and the direct interaction of tau with APP is indicated.[28]

In this study, WAVE was co-accumulated with hyperphosphorylated tau and phosphorylated CRMP2 in neurons of the AD brain, and the interaction between WAVE, CRMP2, and hyperphosphorylated tau was found in the cytosol fraction of AD. Furthermore, three-dimensional analysis confirmed the interaction in the hippocampus of 3xTg-AD mice. In addition, the extent of the intraneuronal accumulation of WAVE was less than that of hyperphosphorylated tau and phosphorylated CRMP2 in brains of AD and 3xTg-AD mice. Thus, these results suggest that tau pathology may induce intraneuronal accumulation of phosphorylated CRMP2, which in turn initiate WAVE accumulation. However, in JNPL3 mice, no WAVE accumulation was detected in neurons showing phosphorylated CRMP2 accumulation. Therefore, the hyperphosphorylation of CRMP2 induced by the pathology of Aβ/APP may be important for subsequent WAVE accumulation. Thus, we suggest that hyperphosphorylation of CRMP2 may be induced by pathology of Aβ/APP, and then intraneuronal accumulation of hyperphosphorylated CRMP2 is mediated by hyperphosphorylated tau. Subsequently, the accumulation of hyperphosphorylated CRMP2 may initiate the accumulation of WAVE in neurons of AD brains (see supplemental Figure S4 at *http://ajp.amjpathol.org*).

A recent study suggested that a direct interaction between tau and actin cytoskeletal network may be a critical mediator of hyperphosphorylated τ-induced neurotoxicity.[29] Furthermore, abnormality of p21-activated kinase, which also regulates actin assembly, is reported in AD brains, and its involvement in Aβ-induced signaling and synaptic deficit has been suggested.[30] Thus, increasing evidence indicates that the disturbance of actin assembly is induced by various mechanisms and is closely related to synaptic dysfunction and neurodegeneration occurs in AD brains. In addition, in our preliminary examination, we found that random and/or aberrant neurite extensions revealed by the F-actin staining were observed during the massive co-expression of phosphorylated tau, phosphorylated CRMP2, and WAVE in rat primary cultured neurons (see supplemental Figure S5 at *http://ajp.amjpathol.org*). Thus, our study supports previous reports suggesting the deficits of actin assembly in AD brains, and provides a novel idea in the pathway of the disturbance of actin cytoskeletons. However, the possibility still remains that WAVE accumulation is only involved as a subset of NFTs that has no effect in the AD pathology. Taken together, we suggest that WAVE accumulation may be involved in the tangle modification by pathology of Aβ/APP, and imply the possible correlation between WAVE accumulation and synaptic deficits mediated by disturbance of actin assembly in AD brains.

Acknowledgments

We thank Dr. Yasuo Ihara (The University of Tokyo, Tokyo, Japan and Doshisha University, Kyoto, Japan) for anti-phosphorylated CRMP2 antibody (clone 3F4). 3xTg-AD mice were kindly provided by Dr. Mark P. Mattson

(National Institute on Aging, Baltimore, MD) and Dr. Frank M. LaFerla (University of California, Irvine, CA). We thank Mr. Daisuke Takamatsu and Mr. Kousuke Imaue for the technical assistance.

References

1. Selkoe DJ: Translating cell biology into therapeutic advances in Alzheimer's disease. Nature 1999, Suppl 399:A23–A31
2. Ihara Y, Nukina N, Miura R, Ogawara M: Phosphorylated tau protein is integrated into paired helical filaments in Alzheimer's disease. J Biochem 1986, 99:1807–1810
3. Gómez-Isla T, Hollister R, West H, Mui S, Growdon JH, Petersen RC, Parisi JE, Hyman BT: Neuronal loss correlates with but exceeds neurofibrillary tangles in Alzheimer's disease. Ann Neurol 1997, 41:17–24
4. McKee AC, Kowall NW, Kosik KS: Microtubular reorganization and dendritic growth response in Alzheimer's disease. Ann Neurol 1989, 26:652–659
5. Rodriguez OC, Schaefer AW, Mandato CA, Forscher P, Bement WM, Waterman-Storer CM: Conserved microtubule-actin interactions in cell movement and morphogenesis. Nat Cell Biol 2003, 5:599–609
6. Pilpel Y, Segal M: Rapid WAVE dynamics in dendritic spines of cultured hippocampal neurons is mediated by actin polymerization. J Neurochem 2005, 95:1401–1410
7. Terry RD, Masliah E, Salmon DP, Butters N, DeTeresa R, Hill R, Hansen LA, Katzman R: Physical basis of cognitive alterations in Alzheimer's disease: synapse loss is the major correlate of cognitive impairment. Ann Neurol 1991, 30:572–580
8. Miki H, Suetsugu S, Takenawa T: WAVE, a novel WASP-family protein involved in actin reorganization induced by Rac. EMBO J 1998, 17:6932–6941
9. Dahl JP, Wang-Dunlop J, Gonzales C, Goad ME, Mark RJ, Kwak SP: Characterization of the WAVE1 knock-out mouse: implications for CNS development. J Neurosci 2003, 23:3343–3352
10. Soderling SH, Langeberg LK, Soderling JA, Davee SM, Simerly R, Raber J, Scott JD: Loss of WAVE-1 causes sensorimotor retardation and reduced learning and memory in mice. Proc Natl Acad Sci USA: 2003, 100:1723–1728
11. Fukata Y, Itoh TJ, Kimura T, Ménager C, Nishimura T, Shiromizu T, Watanabe H, Inagaki N, Iwamatsu A, Hotani H, Kaibuchi K: CRMP-2 binds to tubulin heterodimers to promote microtubule assembly. Nat Cell Biol 2002, 4:583–591
12. Kawano Y, Yoshimura T, Tsuboi D, Kawabata S, Kaneko-Kawano T, Shirataki H, Takenawa T, Kaibuchi K: CRMP-2 is involved in kinesin-1-dependent transport of the Sra-1/WAVE1 complex and axon formation. Mol Cell Biol 2005, 25:9920–9935
13. Yoshida H, Watanabe A, Ihara Y: Collapsin response mediator protein-2 is associated with neurofibrillary tangles in Alzheimer's disease. J Biol Chem 1998, 273:9761–9768
14. Gu Y, Hamajima N, Ihara Y: Neurofibrillary tangle-associated collapsin response mediator protein-2 (CRMP-2) is highly phosphorylated on Thr-509, Ser-518, and Ser-522. Biochemistry 2000, 39:4267–4275
15. Kitamura Y, Shimohama S, Kamoshima W, Ota T, Matsuoka Y, Nomura Y, Smith MA, Perry G, Whitehouse PJ, Taniguchi T: Alteration of proteins regulating apoptosis. Bcl-2, Bcl-x, Bax, Bak, Bad, ICH-1 and CPP32, in Alzheimer's disease. Brain Res 1998, 780:260–269
16. Hasegawa M, Morishima-Kawashima M, Takio K, Suzuki M, Titani K, Ihara Y: Protein sequence and mass spectrometric analyses of tau in the Alzheimer's disease brain. J Biol Chem 1992, 267:17047–17054
17. Oddo S, Caccamo A, Shepherd JD, Murphy MP, Golde TE, Kayed R, Metherate R, Mattson MP, Akbari Y, LaFerla FM: Triple-transgenic model of Alzheimer's disease with plaques and tangles: intracellular Aβ and synaptic dysfunction. Neuron 2003, 39:409–421
18. Hsiao K, Chapman P, Nilsen S, Eckman C, Harigaya Y, Younkin S, Yang F, Cole G: Correlative memory deficits, Aβ elevation, and amyloid plaques in transgenic mice. Science 1996, 274:99–102
19. Lewis J, McGowan E, Rockwood J, Melrose H, Nacharaju P, Van Slegtenhorst M, Gwinn-Hardy K, Paul Murphy M, Baker M, Yu X, Duff K, Hardy J, Corral A, Lin WL, Yen SH, Dickson DW, Davies P, Hutton M: Neurofibrillary tangles, amyotrophy and progressive motor disturbance in mice expressing mutant (P301L) tau protein. Nat Genet 2000, 25:402–405
20. Takata K, Kitamura Y, Tsuchiya D, Kawasaki T, Taniguchi T, Shimohama S: High mobility group box protein-1 inhibits microglial Aβ clearance and enhances Aβ neurotoxicity. J Neurosci Res 2004, 78:880–891
21. Hirata-Fukae C, Li HF, Hoe HS, Gray AJ, Minami SS, Hamada K, Niikura T, Hua F, Tsukagoshi-Nagai H, Horikoshi-Sakuraba Y, Mughal M, Rebeck GW, LaFerla FM, Mattson MP, Iwata N, Saido TC, Klein WL, Duff KE, Aisen PS, Matsuoka Y: Females exhibit more extensive amyloid, but not tau, pathology in an Alzheimer transgenic model. Brain Res 2008, 1216:92–103
22. Arioka M, Tsukamoto M, Ishiguro K, Kato R, Sato K, Imahori K, Uchida T: Tau protein kinase II is involved in the regulation of the normal phosphorylation state of tau protein. J Neurochem 1993, 60:461–468
23. Uchida Y, Ohshima T, Sasaki Y, Suzuki H, Yanai S, Yamashita N, Nakamura F, Takei K, Ihara Y, Mikoshiba K, Kolattukudy P, Honnorat J, Goshima Y: Semaphorin3A signalling is mediated via sequential Cdk5 and GSK3beta phosphorylation of CRMP2: implication of common phosphorylating mechanism underlying axon guidance and Alzheimer's disease. Genes Cells 2005, 10:165–179
24. Ryan KA, Pimplikar SW: Activation of GSK-3 and phosphorylation of CRMP2 in transgenic mice expressing APP intracellular domain. J Cell Biol 2005, 171:327–335
25. Cole AR, Noble W, van Aalten L, Plattner F, Meimaridou R, Hogan D, Taylor M, LaFrancois J, Gunn-Moore F, Verkhratsky A, Oddo S, LaFerla F, Giese KP, Dineley KT, Duff K, Richardson JC, Yan SD, Hanger DP, Allan SM, Sutherland C: Collapsin response mediator protein-2 hyperphosphorylation is an early event in Alzheimer's disease progression. J Neurochem 2007, 103:1132–1144
26. Perry G, Richey PL, Siedlak SL, Smith MA, Mulvihill P, DeWitt DA, Barnett J, Greenberg BD, Kalaria RN: Immunocytochemical evidence that the β-protein precursor is an integral component of neurofibrillary tangles of Alzheimer's disease. Am J Pathol 1993, 143:1586–1593
27. Fein JA, Sokolow S, Miller CA, Vinters HV, Yang F, Cole GM, Gylys KH: Co-localization of amyloid beta and tau pathology in Alzheimer's disease synaptosomes. Am J Pathol 2008, 172:1683–1692
28. Smith MA, Siedlak SL, Richey PL, Mulvihill P, Ghiso J, Frangione B, Tagliavini F, Giaccone G, Bugiani O, Praprotnik D, Kalaria RN, Perry G: Tau protein directly interacts with the amyloid β-protein precursor: implications for Alzheimer's disease. Nat Med 1995, 1:365–369
29. Fulga TA, Elson-Schwab I, Khurana V, Steinhilb ML, Spires TL, Hyman BT, Feany MB: Abnormal bundling and accumulation of F-actin mediates tau-induced neuronal degeneration in vivo. Nat Cell Biol 2007, 9:139–148
30. Ma QL, Yang F, Calon F, Ubeda OJ, Hansen JE, Weisbart RH, Beech W, Frautschy SA, Cole GM: P21-activated kinase aberrant activation and translocation in Alzheimer's disease pathogenesis. J Biol Chem 2008, 283:14132–14143